

VEHICLE STATE AND PARAMETER ESTIMATION BASED ON ADAPTIVE CUBATURE KALMAN FILTER

WEI WANG, SHAOYI BEI, KAI ZHU, LANCHUN ZHANG AND YONGZHI WANG

School of Automotive and Traffic Engineering
Jiangsu University of Technology
No. 1801, Zhongwu Ave., Changzhou 213001, P. R. China
{ nuaawangwei; beishaoyi; zhukaijsut }@126.com; { zhanglanchunnuaa; wangyongzhinuaa }@163.com

Received December 2015; accepted March 2016

ABSTRACT. Acquisition of real-time and accurate vehicle state and parameter information is critical to the research of vehicle chassis control system. However, these key state variables are not easy to measure directly or cheaply. Regarding a 7-DOF non-linear vehicle dynamic mode including Pacejka89 tire model, adaptive cubature Kalman filter based on Sage-Husa noise estimator is proposed to overcome the non-linear model and time-varying noise. The results of virtual experiment proving adaptive cubature Kalman filter (ACKF) algorithm indicate that the estimation precision and anti-noise performance of the ACKF method are superior to unscented Kalman filter (UKF) and extended Kalman filter (EKF) method; therefore, the algorithm is satisfied with the performance of vehicle state estimation.

Keywords: Vehicle dynamics, Pacejka89 tire model, State estimation, Cubature Kalman filter, Adaptive filtering algorithm

1. Introduction. The vehicle state estimation is one of the key technologies of vehicle dynamic control system. Its purpose is acquiring the critical state variables, such as longitudinal velocity, lateral acceleration, yaw rate and other critical parameters. A lack of information of vehicle state and parameters presents a major obstacle for the development of vehicle dynamic control. The effectiveness of vehicle stability control mainly depends on the accuracy of vehicle state and parameter. Currently yaw rate can already be measured by gyro. However, information of sideslip angle has to be acquired through complicated methods such as state estimation and GPS positioning. Among the above two methods, state estimation is easier and more economical than the GPS method. Though some states can be measured by sensors directly, state estimation method is also able to dramatically reduce the interference brought by the measurement noise and process noise contained in the signal [1-4].

Due to the non-linear characteristics of vehicle dynamic model, the extended Kalman filter (EKF) is usually applied to the state estimation. However, after the first-order linear approximation, EKF ignores some of the non-linear characteristics. When the initial error is large, the effect of estimation has a sharp decline and the rate of convergence of filters becomes much slower. In order to further improve the performance of the non-linear estimation, the unscented Kalman filter (UKF) is used for non-linear system state estimation. After unscented transform set of sampling points is transformed to approximate non-linear function probability distribution function, the estimation performance of UKF is better than EKF [5-7]. In order to fulfill the requirements of the vehicle state estimation, it is necessary to study higher precision and more simple ways. The CKF is a new non-linear Gaussian filtering method proposed in recent years. CKF possesses the strict mathematical proof that the numerical integration approximates the weighted Gauss integration by 3-order cubature law. CKF which takes full advantage of cubature

integral value to calculate multi-dimensional integral function has the high efficiency characteristics. CKF possesses the equal volume weight of the $2n$ cubature point (n is the integrand dimension). It proved that the CKF accuracy of the probability distribution approaching nonlinear transformation is better than UKF. However, the CKF accuracy of handling the noise statistical model is not accurate, even when filtering problem occurs with outside influences change [8-10].

For the severe nonlinearity of vehicle estimation model, time-varying of noise statistical characteristics and other issues, the adaptive cubature Kalman filter (ACKF) based on Sage-Husa noise estimator is proposed. The estimation accuracy of UKF, EKF and the proposed ACKF algorithm is comparatively analyzed by the virtual experiment. The results showed that the proposed algorithm has higher precision and strong noise immunity.

2. Vehicle Estimation Model. The 7-DOF non-linear vehicle dynamic model is adopted as the estimation model. The Pacejka89 tire model is used to calculate longitudinal and lateral forces.

2.1. 7-DOF vehicle dynamic model. As shown in Figure 1, it is a 7-DOF non-linear vehicle dynamic model which includes lateral, longitudinal and yaw motions of the vehicle and the rotating motions of the four tires.

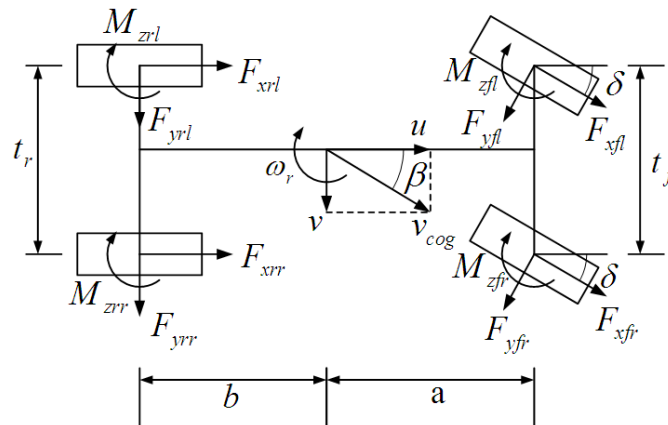


FIGURE 1. 7-DOF non-linear vehicle dynamic model

The equations of vehicle motion are written as

Longitudinal

$$\dot{u} = a_x + v\omega_r \tag{1}$$

$$a_x = (F_{xfl} \cos \delta + F_{xfr} \cos \delta + F_{xrl} + F_{xrr} - F_{yfl} \sin \delta - F_{yfr} \sin \delta) / m \tag{2}$$

Lateral

$$\dot{v} = a_y - u\omega_r \tag{3}$$

$$a_y = (F_{xfl} \sin \delta + F_{xfr} \sin \delta + F_{yfl} \cos \delta + F_{yfr} \cos \delta + F_{yrl} + F_{yrr}) / m \tag{4}$$

Yaw

$$\Gamma = \frac{t_f}{2} \cdot F'_{xfl} - \frac{t_f}{2} F'_{xfr} + \frac{t_r}{2} F_{xrl} - \frac{t_r}{2} F_{xrr} + aF'_{yfl} + aF'_{yfr} - bF_{yrl} - bF_{yrr} + M_{zfl} + M_{zfr} + M_{zrl} + M_{zrr} \tag{5}$$

$$\dot{\omega}_r = \frac{\Gamma}{I_z} \tag{6}$$

where $F'_{xij} = F_{xij} \cos \delta - F_{yij} \sin \delta$, $F'_{yij} = F_{yij} \cos \delta + F_{xij} \sin \delta$.

The vertical forces of each tire are

$$F_{zfl,zfr} = \left(\frac{mg}{2} \pm ma_y \frac{h}{t_f} \right) \frac{b}{l} - \frac{1}{2} ma_x \frac{h}{l} \tag{7}$$

$$F_{zrl,zrr} = \left(\frac{mg}{2} \pm ma_y \frac{h}{t_r} \right) \frac{a}{l} + \frac{1}{2} ma_x \frac{h}{l} \tag{8}$$

The sideslip angle of each tire is given by

$$\alpha_{fl,fr} = \delta - \arctg \frac{v + a\omega_r}{u \pm \frac{t_f}{2}\omega_r} \tag{9}$$

$$\alpha_{rl,rr} = -\arctg \frac{v - b\omega_r}{u \pm \frac{t_r}{2}\omega_r} \tag{10}$$

The side slip angle of the vehicle is

$$\beta = \arctg \frac{v}{u} \tag{11}$$

The tire slip of each tire is written as

$$s_{ij} = \frac{r_e \omega_{ij} - u_{wij}}{u_{wij}} \tag{12}$$

The center velocity of wheel is given by

$$u_{wfl,wfr} = v_{cog} \pm \omega_r \left(\frac{t_f}{2} \mp a\beta \right) \tag{13}$$

$$u_{wrl,wrr} = v_{cog} \pm \omega_r \left(\frac{t_r}{2} \mp b\beta \right) \tag{14}$$

where, u represents the longitudinal velocity, v represents the lateral velocity, v_{cog} represents the vehicle velocity, a_x represents the longitudinal acceleration, a_y represents the lateral acceleration, ω_r represents the yaw rate, β represents the vehicle sideslip angle, Γ represents the yaw moment on z axis, δ represents the steering angle of front tire, F_{xij} represents the longitudinal force of each tire, F_{yij} represents the lateral force of each tire, F_{zij} represents the vertical force of each tire, M_{zij} represents the self-aligning torque of each tire, m represents the vehicle mass, I_z represents vehicle moment of inertia on z axis, a, b are the distances between the center of gravity to the front and the rear axle, $L = a + b$ represents the distances between the front and the rear axle, t_f, t_r are the distances between the left and the right tire, respectively, h represents the height of the center of gravity, α_{ij} represents the sideslip angle of each tire, s_{ij} represents the tire slip of each tire, r_e represents the effective rolling radius, ω_{ij} represents the yaw rate of wheel, and u_{wij} represents the center velocity of wheel.

2.2. Tire model. Pacejka non-linear tire model is applied. The input variables of this model contain vertical load, slip angle and tire slip. Lateral force, longitudinal force and self-aligning torque of each tire can be calculated from unified Equations (15)-(17).

$$y(x) = D \sin(C \arctg(Bx - E(Bx - \arctg Bx))) \tag{15}$$

$$Y(X) = y(x) + s_v \tag{16}$$

$$x = X + s_h \tag{17}$$

where the output variable Y in Equation (16) represents tire side force F_x , tire longitudinal force F_y , and tire self-aligning torque M_z in different cases. The input variable X in Equation (17) represents the tire slip S (when calculating longitudinal force) and tire sideslip angle α (when calculating lateral and self-aligning torque). The expressions of parameters B, C, D, E, s_v, s_h in Equation (15) can be seen in [10]. In the paper, under vertical load of 3.16KN, the related parameters of tire model are valued as $B = 0.237, C = 1.65, D = 3610.5, E = 0.707, s_v = 40.379, s_h = 0.0473$.

2.3. Noise contained non-linear vehicle system. State vector of 7-DOF non-linear vehicle dynamic model is written as:

$$x^s = [u, v, a_x, a_y, \omega_r, \beta, \Gamma]^T \tag{18}$$

Input of system is

$$u = [\delta, \omega_{fl}, \omega_{fr}, \omega_{rl}, \omega_{rr}]^T \tag{19}$$

Observation vector is

$$y = [\omega_r, a_y, u]^T \tag{20}$$

3. Estimation Method Based on ACKF. When the system has inaccurate noise statistical characteristics or time-varying noise, the estimation accuracy of CKF becomes much lower or more divergent. CKF uses Sage-Husa noise estimator estimating noise in order to establish ACKF algorithms. When average value of the process and measurement noise is zero, the variance estimates of Sage-Husa noise estimator respectively are written as

$$\hat{Q}_k = \frac{1}{k} \sum_{j=1}^k (\hat{x}_j - \hat{x}_j^-) (\hat{x}_j - \hat{x}_j^-)^T \tag{21}$$

$$\hat{R}_k = \frac{1}{k} \sum_{j=1}^k (z_j - \hat{z}_j^-) (z_j - \hat{z}_j^-)^T \tag{22}$$

Here, $\hat{x}_j = \hat{x}_j^- + K\varepsilon_j$, and $\varepsilon_j = z_j - \hat{z}_j^-$. K is the gain of filter; therefore, Equation (21) can be written as

$$\hat{Q}_k = \frac{1}{k} \sum_{j=1}^k K\varepsilon_j\varepsilon_j^T K^T \tag{23}$$

Here, $E[\varepsilon_j, \varepsilon_j^T] = P_{zz,j}$. Either side of Equation (23) is taken desired. It can be expressed as the following

$$E[\hat{Q}_k] = \frac{1}{k} \sum_{j=1}^k P_j^- - P_j = \frac{1}{k} \sum_{j=1}^k \left(\frac{1}{2n} \sum_{i=1}^{2n} X_{i,k}^* X_{i,k}^{*T} - \hat{x}_k^- \hat{x}_k^{-T} - P_j \right) + Q_k \tag{24}$$

\hat{Q}_k is given as the following

$$\hat{Q}_k = \frac{1}{k} \sum_{j=1}^k \left(K\varepsilon_j\varepsilon_j^T K^T - \frac{1}{2n} \sum_{i=1}^{2n} X_{i,k}^* X_{i,k}^{*T} + \hat{x}_k^- \hat{x}_k^{-T} + P_j \right) \tag{25}$$

Then, the recursive form of \hat{Q}_k is

$$\hat{Q}_k = \left(1 - \frac{1}{k} \right) \hat{Q}_{k-1} + \frac{1}{k} \left(K\varepsilon_j\varepsilon_j^T K^T - \frac{1}{2n} \sum_{i=1}^{2n} X_{i,k}^* X_{i,k}^{*T} + \hat{x}_k^- \hat{x}_k^{-T} + P_k \right) \tag{26}$$

\hat{R}_k is given as the following

$$\hat{R}_k = \frac{1}{k} \sum_{j=1}^k \varepsilon_j\varepsilon_j^T = \frac{1}{k} \sum_{j=1}^k P_{zz} = \frac{1}{k} \sum_{j=1}^k \left(\frac{1}{2n} \sum_{i=1}^{2n} Z_{i,k} Z_{i,k}^T - \hat{z}_k^- \hat{z}_k^{-T} \right) + R_k \tag{27}$$

Then, the recursive form of \hat{R}_k is

$$\hat{R}_k = \left(1 - \frac{1}{k} \right) \hat{R}_{k-1} + \frac{1}{k} \left(\varepsilon_k\varepsilon_k^T - \frac{1}{2n} \sum_{i=1}^{2n} Z_{i,k} Z_{i,k}^T + \hat{z}_k^- \hat{z}_k^{-T} \right) \tag{28}$$

The memory index d_{k-1} can be expressed as the following, similar to Sage-Husa time-varying noise estimate method.

$$\hat{Q}_k = (1 - d_{k-1}) \hat{Q}_{k-1} + d_{k-1} \left(K \varepsilon_j \varepsilon_j^T K^T - \frac{1}{2n} \sum_{i=1}^{2n} X_{i,k}^* X_{i,k}^{*T} + \hat{x}_k^- \hat{x}_k^{-T} + P_j \right) \quad (29)$$

$$\hat{R}_k = (1 - d_{k-1}) \hat{R}_{k-1} + d_{k-1} \left(\varepsilon_k \varepsilon_k^T - \frac{1}{2n} \sum_{i=1}^{2n} Z_{i,k} Z_{i,k}^T + \hat{z}_k^- \hat{z}_k^{-T} \right) \quad (30)$$

where, $d_{k-1} = \frac{1-b}{1-b^k}$, the b is forgetting-factor, the value is given in $[0.95, 0.995]$.

In CKF algorithm, the covariance matrix of process noise and measuring noise is calculated in Equation (29) and Equation (30), and thus, the ACKF is obtained.

4. Experimental Verification Based on ADAMS. To verify the proposed algorithm, the virtual experiment is conducted on ADAMS. Parameters of the vehicle are: $m = 1685\text{kg}$, $I_z = 2580\text{kg}\cdot\text{m}^2$, $a = 1.16\text{m}$, $b = 1.36\text{m}$, $t_f = 1.54\text{m}$, $t_r = 1.59\text{m}$, $h = 0.436\text{m}$, $r_e = 0.36\text{m}$. ADAMS full vehicle model is composed of front and rear suspension subsystem, body subsystem, steering subsystem, braking subsystem, front and rear tire subsystems. Establish input and output “communicator” between subsystems. Tire model is the Pac89 tire model contained in the ADAMS software. The assembled ADAMS vehicle model is shown in Figure 2.



FIGURE 2. Full vehicle model

Under extreme condition in ADAMS, to simulate the extreme conditions vehicle handling response, vehicle travels along the double lane path. The whole operation period is 10s, and sampling time is 0.01s.

In the state estimation, process noise is set as a zero-mean white Gaussian noise sequence, and the covariance matrix is given by

$$\hat{Q}_k = 0.01 \cdot |\max(state(i)) - \min(state(i))| \cdot \sin\left(\frac{\pi}{10}t\right) \quad (i = 1, \dots, 7, 0 \leq t \leq 10) \quad (31)$$

where, $\max(state(i))$ and $\min(state(i))$ are the maximum and the minimum values of the i th state parameter during the whole period, respectively.

Covariance matrix of measurement noise is set as a zero-mean white Gaussian noise sequence, the covariance matrix is given by

$$\hat{R}_k = 0.05 \cdot |\max(y) - \min(y)| \cdot \sin\left(\frac{\pi}{10}t\right) \quad 0 \leq t \leq 10 \quad (32)$$

Figure 3 is a comparison between the estimated and experimental values of six key state parameters u , v , a_x , a_y , ω_r , β by three algorithms ACKF, EKF, UKF.

As shown in Figure 3, the estimation accuracy of ACKF algorithm is higher than that of UKF and EKF. In Figure 3(c), the estimation accuracy of the longitudinal acceleration of three algorithms has obvious differences, and the estimation error of EKF is higher than that of others. In Figure 3(e), because the model applies inaccurate initial parameters, and EKF algorithm does not contain parameter correcting estimator, the accuracy of EKF

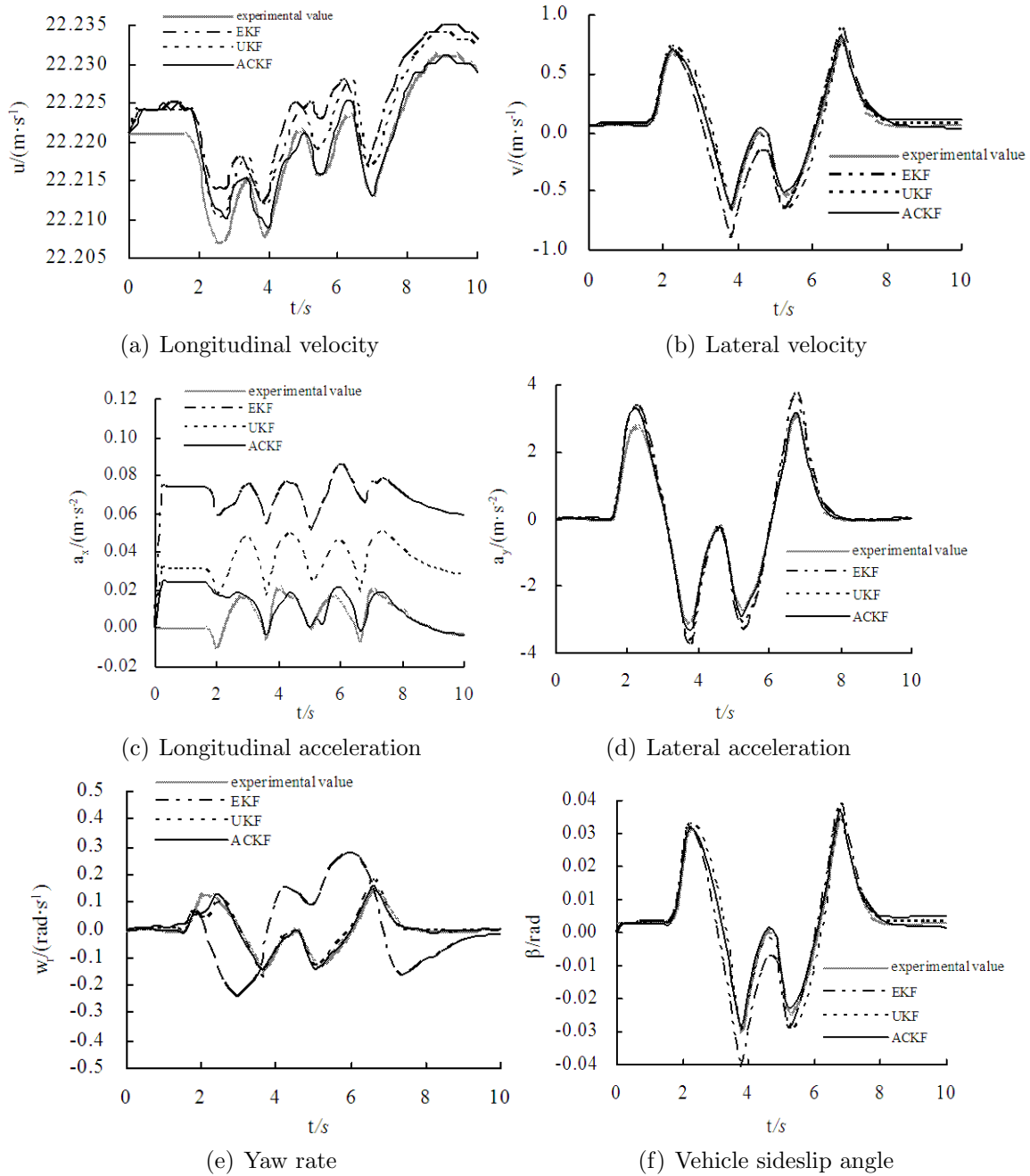


FIGURE 3. Comparison between estimated and virtual experiment values (double lane)

is apparently lower than that of UKF and ACKF, and even the values become seriously distorted in the estimation of yaw rate.

To have a quantitative comparison between the three algorithms, Table 1 gives the mean absolute error (MAE) and the root mean square error (RMSE) of each algorithm.

As shown in Table 1, under the same circumstance, the estimation accuracy of ACKF is higher than that of the other two algorithms.

5. Conclusion.

(1) This work proposed ACKF and applied it into the vehicle states and parameters estimation. The ACKF combines CKF and Sage-Husa noise estimator. Therefore, the algorithm is able to conduct states and parameters parallel estimation of a non-linear system containing inaccurate model parameters and time-varying noise.

TABLE 1. MAE and RMSE of each algorithm

Evaluation	State parameter	EKF	UKF	ACKF
MAE	u (m/s)	0.00452	0.0035	0.00136
	v (m/s)	0.0687	0.0463	0.0261
	a_x (m/s ²)	0.0669	0.0345	0.0105
	a_y (m/s ²)	0.226	0.192	0.145
	ω_r (rad/s)	0.126	0.0115	0.00765
	β (rad)	0.00304	0.00211	0.00109
RMSE	u (m/s)	0.0047	0.00325	0.0018
	v (m/s)	0.099	0.0664	0.0278
	a_x (m/s ²)	0.0657	0.0352	0.0165
	a_y (m/s ²)	0.339	0.247	0.147
	ω_r (rad/s)	0.256	0.0212	0.0128
	β (rad)	0.00436	0.00299	0.00129

(2) Under the ADAMS high speed extreme driving condition, ACKF which is compared to UKF and EKF has higher estimation accuracy and stronger anti-noise performance for the case when the measurement system has time-varying noise characteristics. ACKF can estimate accurately vehicle states and parameters.

(3) The idea to integrate ACKF algorithm with vehicle key state parameter estimation can provide theoretical guide to the software design of the estimator in the vehicle automatic control system.

Acknowledgment. This work is partially supported by the National Science Foundation of China (Grant No. 51305175), the National Science Foundation of Jiangsu Province (Grant No. BK2012586), the National Science Foundation of Jiangsu University of Technology (Grant No. KYY14041), the 333 Project of Jiangsu Province (BRA2015365) and Jiangsu Province “Six Personnel Peak” Fund Projects (Grant No. 2012-ZBZZ-023) and (Grant No. 2013-ZBZZ-039). The authors also gratefully acknowledge the helpful comments and suggestions of the reviewers, which have improved the presentation.

REFERENCES

- [1] H. W. Son, A study on design of a robust vehicle side-slip angle observer using an integration of kinematic and bicycle model, *KSAE Annual Conference*, Daejeon, Korea, 2008.
- [2] A. Y. Ungoren, H. Peng and H. E. Tseng, A study on lateral speed estimation methods, *Int. J. Vehicle Autonomous Systems*, vol.2, pp.126-144, 2004.
- [3] S. H. You, J. O. Hahn and H. C. Lee, New adaptive approaches to real-time estimation of vehicle slidslip angle, *Control Engineering Practice*, vol.17, no.12, pp.1367-1379, 2009.
- [4] D. Maessen and E. Gill, Relative state estimation and observability analysis for formation flying satellites, *Journal of Guidance, Control, and Dynamics*, vol.35, no.1, pp.321-326, 2012.
- [5] S. J. Julier, J. K. Uhlmann and H. F. Durrant-Whyte, New approach for filtering nonlinear systems, *Proc. of the American Control Conference*, pp.1628-1632, 1995.
- [6] A. Giannitrapani, N. Ceccarelli and F. Scortecci, Comparison of EKF and UKF for spacecraft localization via angle measurements, *IEEE Trans. Aerospace and Electronic Systems*, vol.47, no.1, pp.75-84, 2011.
- [7] F. Gunnarsson, N. Bergman and U. Forssell, Particle filters for positioning, navigation, and tracking, *IEEE Trans. Signal Processing*, vol.50, no.2, pp.425-437, 2002.
- [8] I. Arasaratnam and S. Haykin, Cubature Kalman filters, *IEEE Trans. Automatic Control*, vol.54, no.6, pp.1254-1269, 2009.
- [9] J. Dakhlallah, S. Glaser and S. Mammar, Tire-road forces estimation using extended Kalman filter and sideslip angle evaluation, *American Control Conference*, Seattle, USA, pp.4597-4602, 2008.
- [10] M. C. Best, A. P. Newton and S. Tuplin, The identifying extended Kalman filter: Parametric system identification of a vehicle handling model, *Proc. of IMechE, Part K: Journal of Multi-body Dynamics*, vol.211, no.1, pp.87-98, 2007.